Editors' Suggestion

Sluggish diffusion in random equimolar FCC alloys

Murray S. Daw[1,*] and Michael Chandross[2]

[1]*Department of Physics and Astronomy, Clemson University Clemson, South Carolina 29634, USA*

[2]*Material, Physical, and Chemical Sciences Center, Sandia National Laboratories Albuquerque, New Mexico 87123, USA*

(Received 14 December 2020; accepted 16 February 2021; published 9 April 2021)

We examine vacancy-assisted diffusion in the 57 random, equimolar alloys that can be formed from Cu, Ag, Au, Ni, Pd, and Pt based on the well-tested embedded atom method functions of Foiles, Baskes, and Daw [Phys. Rev. B **33**, 7983 (1986)]. We address the suggestion [Yeh *et al.*, Adv. Eng. Mater. **6**, 299 (2004)] that increasing the number of constituents causes diffusion to be "sluggish" in random, equimolar alloys. Using molecular dynamics (MD) simulations of random alloys with a single vacancy, combined with calculations of vacancy formation, we extract vacancy-assisted diffusivities in each alloy. After developing and applying several possible criteria for evaluating "sluggishness," we find that only a small minority (from 1 to 8, depending on how sluggishness is defined) of the alloys exhibit sluggish diffusion whereas in the large majority of alloys diffusion is faster and in quite a few cases ought to be considered vigorous (that is, faster than in any of the constituents). We correlate diffusivity with a combination of the mean of the constituent diffusivity and a simple function of lattice mismatch. We conclude that simply increasing the number of constituents in such alloys does *not* systematically alter the diffusion, but that instead lattice mismatch plays a primary factor; sluggish diffusion is more likely to occur in a window of small lattice mismatch (1–3%) even in binary alloys. Quantitatively, our calculated diffusivities correlate with a combination of (1) rule of mixtures of the diffusivities of the constituents, and (2) a simple function of the lattice mismatch; this accounts for the large majority of our calculated diffusivities to within a factor of 2 (over a range of three orders of magnitude). We also find that while lattice mismatch on the order of 1–3% is necessary for sluggish diffusion, it is not sufficient.

DOI: 10.1103/PhysRevMaterials.5.043603

I. INTRODUCTION

The hypothesis that a random alloy formed from equal amounts of many constituents, often referred to as compositionally complex alloys (CCAs) or high entropy alloys (HEAs), would exhibit sluggish diffusion seems to have originated from a suggestion based on intuition [1–4]. That intuition and other related ideas about "core effects" led to the investigation of the actual properties of HEAs, with the result that many such alloys have been made and tested and some have shown decidedly favorable properties (see Ref. [5] and references therein). Following those discoveries, there have been more principled investigations—both experimental and theoretical—of the sluggish diffusion hypothesis and the other core HEA effects. This paper reports a systematic theoretical investigation into the nature of vacancy-assisted diffusion in random, equimolar alloys in order to determine the often complex relationship between composition and diffusion.

A. Experimental literature and use of homologous temperature

In one of the first (and certainly one of the most cited) papers on this subject, Tsai, Tsai, and Yeh [6] ("TTY13" in the following) reported measurements of diffusivity in a five component FCC, solid-solution-like alloy (CoCrFeMnNi). They analyzed those measurements with a "quasibinary" approach and extracted pre-exponentials and activation energies for each of the elements. They also set out to compare the tracer diffusivities for each constituent to the values in other hosts (pure metals and alloys). For this comparison, they argued for the use of homologous values (that is, evaluating the diffusivity extrapolated to the melt or solidus for each host, or equivalently by scaling the activation energy by the melting or solidus temperature). Their reason for using homologous values was stated simply and briefly: "the activation energies are usually linearly related to the melting points of the matrix (host)" [7]. They found that the normalized activation energy (Q/T_{melt}) for each of the constituents correlated positively with the number of components in the alloys considered, and this was then their confirmation of "sluggish diffusion"

Miracle [9] traced the mixed experimental evidence for and against sluggish diffusion in HEAs, including the use of homologous temperature. He pointed out that on a straight comparison at the same absolute temperature, the diffusion in many multicomponent systems is actually faster than in simpler alloys. He also noted that the conclusion that the diffusivity is positively correlated with the number of constituents may be true for a limited set, but when he broadened the data set to include more elements and alloys he showed that HEAs are, in fact, slower than average, although not the slowest compared with other FCC elements and alloys. In the larger set he investigated, the slowest (again, extrapolated to the corresponding melting point) are two pure elements (Pb and Pt)

*Corresponding author: daw@clemson.edu

and four binaries (Cr-Ni, Ni-W, Cu-Pt, and Ni-Cu). Miracle concluded that HEAs are not "anomalous" or even "unusual" or "exceptional" in their diffusive behavior in comparison to elements and simpler alloys, *even when judged based on homologous temperature.* Finally, he pointed to the need for more robust analysis of the atomistic processes involved, such as what is presented here.

We note that there are two separate themes that run through the literature on sluggish diffusion: (1) whether a random alloy with equal amounts of multiple components might be expected to show slower diffusion, and (2) whether comparisons between hosts should use homologous rather than absolute temperature. These are separate, if related, issues and it is instructive to approach these questions separately to the extent that it is possible.

B. Theoretical investigations

Complimentary to the experiments, the authors of TTY13 also proposed a theoretical analysis based on the complexity of a multicomponent alloy. They argued for the existence of "traps" that can pin an atom to a particular location, thereby inhibiting diffusion. The traps occur randomly from variations in bond strength and bond length in the interactions between various atomic pairs. They supported this by a simple nearest-neighbor bond-counting argument in which the effects due to variations in bond strength and bond length are lumped together into empirical parameters. They conclude (without rigorous proof) that increasing the number of constituents should increase the sluggishness of the diffusion. This approach uses more detailed reasoning than the basically intuitive suggestion behind the original hypothesis.

However, the correlation of sluggishness with increasing number of constituents proposed by TTY13 is not borne out by the available experimental data (see [9]). Some alloys exhibit slower diffusion and others do not, and there is no apparent correlation with number of elements. In other words, the observed cases of sluggish diffusion in some alloys would seem to depend on *a specific cause beyond* the presence of many constituents.

Furthermore, the analysis in TTY13 is oversimplified because migration barriers involve the difference of two energies, namely the energy of a local basin and the energy of the saddle point transition to another basin. In the case of vacancy-assisted diffusion, the saddle point usually corresponds to a migrating atom squeezing through a narrow pass on its way to occupy a nearby vacant site. The analysis in TTY13 considers variations in the *local basin energetics* caused by random mixing of atomic types that they reasoned includes variations of bond strength and bond length. By contrast, their analysis uses the unjustified assumption that the saddle point energy is the *same throughout the material, and independent of the type of migrating atom or its neighbors*. Finally, they do not clearly account for or discuss the effect of the local basin energetics on vacancy concentrations. Obviously, vacancy concentration is an important factor in vacancy-assisted diffusion, and a thorough comparison of diffusivities must take this into account or otherwise justify why not. The approach in TTY13 is clearly an oversimplification and a deeper analysis is called for.

Choi *et al.* [10] took a step in the direction of a deeper analysis by calculating migration barriers for motion of a vacancy in a five-component alloy (CoCrFeMnNi) modeled with second-nearest-neighbor modified embedded atom method (MEAM) potential. They cataloged a number of different barriers and showed an overall distribution by type of migrating atom. Though the sampling was very limited it did seem to show some features in agreement with experimental data.

More reliable energetics are expected from first-principles calculations (see Ref. [11] for NiCoCr and NiCoFeCr and Ref. [12] for CrMnFeCoNi) where they consider vacancy motion among several tens of neighboring configurations in order to determine a distribution of barriers for a vacancy exchanging with different types. The results are somewhat in agreement with experimental data and also with the MEAM calculations discussed in the previous paragraph. These two theoretical investigations, however, have been limited to a small set of alloys and neither offers much additional insight into the general hypothesis of sluggish diffusion.

A more robust investigation related to the current report is the recent work of Bonny *et al.* [13], that reports a study of tracer diffusivities in various four-component alloys (made from Ni, Fe, Cr, and Pd) studied using tailored EAM potentials [14]. The migration barriers were calculated for a large set of local configurations and entered into a training and validation set for an artificial neural network that was then implemented into an atomic kinetic Monte Carlo calculation. The result is a deeper study of the effects of configurational randomness in a set of four-component alloys on vacancy mobility. They concluded that the diffusivities are *higher* in the alloys studied with increasing number of constituents, directly contradicting the sluggish hypothesis. They make no attempt to reconcile their calculations with experimental observations of sluggish diffusion in some alloys, and the authors call for a "deeper and systematic study" of diffusion in multicomponent alloys.

Another recent work [15] investigated the vacancy mobility in disordered FCC Ni-Fe alloys by combining MD and Monte Carlo methods using EAM potentials [14]. They found that the vacancy mobility was a minimum (below the mobility in the pure elements) at 20% Fe, which was tied to the percolation threshold for the faster species (Fe). Based on this they also speculated that increasing the number of components to five ought to produce an optimally sluggish alloy because each of the components would be at the same percolation limit of 20%.

Similar techniques were employed to study the effect on vacancy mobility of compositional ordering in Ni-Fe alloys [16], based on some first-principles calculations and also on EAM potentials [14]. Similar to the minimum vacancy mobility observed in Ni-20% Fe, the ordered $L1_2$-Ni_3 Fe structure showed the lowest mobility among the structures considered, with the vacancy found dominantly on the Fe sublattice. The suppression of vacancy hopping in the ordered structures was attributed to a lower effective attempt frequency associated with fewer configurationally suitable exits for the vacancy. The results suggest that in samples that are nominally disordered, any buildup of local ordering may inhibit vacancy mobility.

C. The plan of this work

Our goal is to theoretically investigate the vacancy-assisted diffusion in random, equimolar alloys with varying numbers of constituents to determine if there is a negative correlation between number of constituents and diffusion. Specifically, we choose to investigate diffusion assisted by single vacancies in a single crystal, thereby avoiding the complications of vacancy complexes or diffusion along grain boundaries. We analyze the results both in terms of absolute diffusivity and also homologous values. We also investigate correlations between the constituent properties and the resulting diffusivity in the alloys.

We have chosen to focus on "fully random alloys" (in the words of TTY13), so as to key in on that part of the "sluggish" hypothesis: *increasing the number of components in fully random alloys suppresses diffusion*. It may well be experimentally that nominally disordered alloys have in fact developed some local degree of ordering or clustering. In that case, it is to be expected that the *loss of randomness* (either to clustering or ordering of the components) will affect the diffusivity, but this is not what is described in TTY13. So, for the present, we leave questions of deviations from random for a later investigation, and instead focus the present investigation on perfectly random alloys.

Random alloys offer intrinsic difficulties for theoretical atomic-scale analysis. Electronic structure calculations like local density approximation are highly accurate and can study complex configurations but are, of course, limited in cell size and simulation time. Semiempirical methods like EAM [17] are significantly less computationally demanding at the trade-off of some accuracy, but are challenged by the initial lead time required for fitting potentials to target properties of multicomponent systems. We avoid this lead time by using an existing, well-tested [18–20] set of potentials for a multicomponent system of FCC metals. We argue that one does not need a perfect set of EAM functions to address that question at a generic level, but rather sluggish diffusion is being proposed on *general grounds* and therefore should be testable with any reasonable set of semiempirical potentials.

In the present work, we chose an existing set of EAM potentials to study alloys formed from among six FCC constituents, greatly increasing the number of possible equimolar alloys compared to previous work. For example, the four-component set of functions in Ref. [13] would permit 11 random equimolar alloys to be studied, whereas in this work, the set of six constituents widens this to 57 unique random equimolar alloys. We also deepen the analysis of the diffusion mechanism by correlating with various properties of the constituents. As discussed above, we analyze our results first with absolute temperature and then with homologous temperature, in order to isolate the effects of the number of constituents, and clearly separate it from the use of homologous values.

Our approach examines two parallel paths. First, because the vacancy diffuses at least as fast as any individual element, we examine the diffusion of the vacancy itself, irrespective of the motions of the individual constituents, to determine if it is less mobile in multicomponent alloys. Second, we refine the analysis by tracking the diffusion of each of the six elements in the various hosts (formed from that element and others in the set), to see if the trend seen for the vacancy generally holds for individual elements.

A complete analysis of diffusivity in alloys must include both formation and migration energies [21]. In general, the measure of the rate of vacancy-assisted self-diffusion is a combination of vacancy concentration and vacancy mobility:

$$D = cM. \tag{1}$$

The concentration is expected to have an Arrhenius form and is associated with a vacancy formation energy,

$$c(T) = \exp\Big[-\frac{Q_f}{k_B T}\Big]. \tag{2}$$

The mobility is also Arrhenius,

$$M(T) = M_0 \exp\Big[-\frac{Q_m}{k_B T}\Big] \tag{3}$$

so that the activation energy for diffusion is the sum of formation and migration,

$$Q_d = Q_f + Q_m. \tag{4}$$

The activation energies and the preexponential are functions of composition. Furthermore, tracer diffusivity is similarly expected to show Arrhenius behavior, with the activation energies specific to each component and host. In this work we calculate both formation and migration energies as functions of composition.

Our definition of sluggish diffusion needs to be made more concrete. Is there a definition for sluggish which will serve all circumstances (for example, recrystallization as contrasted with phase separation)? Is mobility the key factor, or diffusivity? Is the diffusivity (at a given temperature) or the activation energy for diffusion a more appropriate measure? Having evaluated some property of the alloy, what should it be compared to? In analyzing our results, we consider several possible criteria by which one might evaluate whether diffusion in a particular alloy is "sluggish," some of which are more stringent than others. The end result is that we do find a small number of alloys from our set that, even by the most stringent criterion, could reasonably be called sluggish, but a larger set of alloys that are the opposite (quite vigorous). Furthermore, the search for reasonable criteria suggests a general means of analyzing diffusion in alloys that has led to significant correlations in our calculated diffusivities with both diffusivities of the pure constituents and lattice mismatch among the constituents. This broadens the scope of this paper beyond the specific evaluation of the sluggish hypothesis.

This paper is organized as follows. In Sec. II we discuss the methods used to calculate the vacancy concentration and mobility factors in random equimolar alloys and our means of making comparisons among them. Section III presents results of the self-diffusion where we show that the number of constituents is not the determining factor, but rather the lattice mismatch. Section IV presents corresponding results of tracer diffusivities, compares to experiments, and draws the same conclusions. Finally, we summarize our conclusions in Sec. V.

TABLE I. Computed values for the activation energy for diffusion ($Q_d = Q_f + Q_m$) compared to available thermochemical data.

Element	Q_d (eV) (this work)	Q_d (eV) (experiment)
Cu	1.95	2.13
Ag	1.74	1.82
Au	1.68	1.83
		1.97 [29]
Ni	2.68	2.97
		2.81 [30]
Pd	2.18	2.90
Pt	2.50	2.71 [26]

II. METHODS

A. Semiempirical potentials

We used the well-tested functions of Foiles, Baskes, and Daw [19,20] (hereafter FBD), developed for the elements Cu, Ag, Au, Ni, Pd, and Pt, and dilute binary alloys formed from them. The FBD potentials were fitted to sublimation energy, lattice constant, elastic constants, and vacancy formation energies of the elements, as well as the dilute heats of alloying for all of the binaries. The vacancy migration energies were calculated after the fit and constitute a test of the EAM. We show that the general, approximate relation $Q_f/Q_m = 2$ for the pure elements carries over to the alloys as well. The FBD functions have been used in many studies [18] and have proven to be robust and reliable. The melting points for the elements in this set have been carefully calculated [22] and will be of use in the present study. The present calculation of alloying effects on diffusivity takes us further away from the data used to train and initially test the functions.

In FBD, the experimental vacancy formation energy was included in the original training set for the functions, and the disagreement with experiment was as large as 0.2 eV with an average of 0.05 eV over the set. A comparison to experimental values for vacancy migration energies was used as a test of the functions after fitting; the disagreement with these experiment values was as large as 0.6 eV but on average was 0.14 eV. In combining vacancy formation and migration energies to get the full activation energy for diffusivity, we can compare to experimental diffusion energies. Based on the known discrepancies in formation and migration energies, we expect that the disagreement with experimental diffusion energies could average about 0.2 eV. In Table I we present the comparison to available thermochemical data. The average discrepancy between our calculations and these experimental data is 0.3 eV, with Pd showing the largest discrepancy (0.7 eV). Note that these results are not new in that they involve properties of pure elements that have been evaluated in previous publications. We show these here by comparison to thermochemical data in order to help calibrate our expectations later when we compare our results for alloys to the same thermochemical database.

B. Vacancy formation energies

The assumption of randomness in HEAs can be expressed formally by considering averages over an ensemble of systems with equal probability for any and all assignment of types (consistent with overall composition) on the underlying FCC lattice. The following simple argument shows how this can be carried out. We begin with a large cell (no vacancies) of N atoms, with all sites occupied by the same number of various types so that the composition is equimolar. Now make N-2 copies of that cell (for a total of N-1 cells), and put them together to form a larger solid from those cells for a total of $N(N\text{-}1)$ atoms with $N(N\text{-}1)$ sites (that is, all sites occupied). Next we form a new solid in a particular way so as to form a representative sampling of the possible vacancies but with the same number of atoms (hence more sites). From each cell take a different atom: from cell no. 1 take atom no. 1, and from cell no. 2 take atom no. 2, etc., and so leaving a vacancy on a unique site in each cell. The last cell, numbered (N-1), has lost an atom at site (N-1). The atoms removed can be put together to form a new cell (which will be given number N), and because those atoms are a complete sampling of the atoms from the original cell *except for the last site N*, the *new* cell will have only N-1 atoms, with no atom on the Nth site. So, we now have N cells, each with N-1 atoms and 1 vacancy (on site i in cell i), which are put together to form a solid. This defective solid has $N(N\text{-}1)$ atoms in it and also N vacancies (for N^2 sites total). The defective solid has larger volume, but at zero pressure this does not contribute to the energetics. The total energy required to make this representative sampling of vacancies from the perfect lattice is ΔE, and will be extrinsic (that is, increasing with N). Having created N vacancies, the vacancy formation energy (Q_f) is then $\Delta E/N$. Using this procedure, we have calculated Q_f for cells of 256 atoms and random alloys with from two to six components. The results have been compared for various different random assignments of the types on the sites, and are converged in this regard to better than 0.01 eV.

C. Vacancy and atomic mobilities

The EAM calculations for vacancy hopping are carried out in molecular dynamics (MD) using the mean-square-displacement (MSD) of all atoms, as done before, for example, by de Lorenzi and Ercolessi [27]. All calculations used LAMMPS [28]. Periodic cells were constructed with as close to equimolar compositions as possible for the given total number of atoms. The coefficient of thermal expansion (CTE) was calculated for each cell and composition by equilibrating and averaging using *NPT* dynamics in LAMMPS. This CTE is used to expand the cell to an appropriate volume for the desired temperature, and this is followed by deleting an atom, equilibrating with Langevin dynamics, and finally running under *NVE* dynamics while collecting the displacement data. During the MD run, the atoms displace, some moving significantly, and this diffusion is aided by the absence of the deleted atom (i.e., by the "presence" of a vacancy). We also average over which atom is deleted.

The value from a single run for the mobility is given [27] by tracking the mean-squared displacement (MSD),

$$\mathrm{MSD}(t) = \langle |\vec{u}(t)|^2 \rangle, \tag{5}$$

where $\vec{u}(t) = \vec{r}(t) - \vec{r}(0)$ is the displacement of an atom at time t from the beginning of the run, and the angle brackets indicate an average over all atoms. For long times the MSD

is linear in time with slope $6\tilde{M}$, where $\tilde{M}$ is the average vacancy mobility. This calculated factor is proportional to the concentration of vacancies, so that the total vacancy mobility is then $M = N_{\text{at}}\tilde{M}$, where N_{at} is the number of atoms in the simulation. In the rest of this paper we report the vacancy mobility M, which is independent of the number of atoms in the cell. The extension to tracer mobilities and diffusivities is straightforward, in that the MSD [Eq. (5)] is restricted to atoms of a particular type.

For each temperature, a single configuration is created by deleting one atom from a cell at random, and running as above for a time long enough to give a good sampling of the diffusion (to be discussed more below). At each temperature, at least 256 (occasionally up to 1024 for validation) configurations are run independently (i.e., a different deleted atom and different seeds for the velocity generation prior to thermalization) and the values of M are then averaged to give the calculated value for that composition at that temperature. We have performed calculations for cells of 108 and 256 atoms, and confirmed that our calculated values of M do not depend on cell size.

The appropriate simulation time for each sample depends on the temperature and composition. We first estimate a value of the diffusivity, from approximate values of M_0 and Q_m. The series of calculations begins with the pure elements. In these cases, the activation energies are known, but an estimate of M_0 is required. However, only a few calculations are enough to improve the guess significantly, and we then calculate the diffusivities for the pure elements. The next set of calculations is for alloys. Estimates for alloy mobility are given by an arithmetic average of the migration energies for the constituent elements and a geometric mean of their corresponding preexponentials. (We will show in the next section that this gives a reasonable lower-bound estimate of the alloy diffusivity.) Using this estimate, simulations were initially carried out for a time $t = \lambda^2/M$ where λ (the diffusion length) is set at $3a_0$ (for a_0 the lattice constant of the alloy). After performing a set of calculations at temperatures at approximately 50-K intervals, the M are fitted to an Arrhenius form, giving an improved value of M_0 and Q_m. Those values are then used to reevaluate the diffusion length, and the set is redone with longer times if $\lambda < 3a_0$. For the lowest temperatures we studied ($\sim$700 K), this led to a total simulation time (counting all independent samples) of $\sim$5 microseconds. At higher temperatures, the required simulation time is much smaller. We have run spot checks on various calculations by running 100 times longer and found no significant changes in the results.

We use the Arrhenius fit to help measure the statistical errors of the sampling. We first assume that deviations from Arrhenius are due entirely to statistical sampling error. Next we note that the run time t at each temperature was chosen to make the diffusion length $\sqrt{Mt}$ close to the same value independent of temperature. This means that the sampling error in M (related to the number of jumps) is proportional to the value of M itself. In other words, the error distribution in $\ln(M)$ is independent of temperature. Thus, we can write for each sample M_i

$$\ln(M_i) = \ln(M_0) - \frac{Q_m}{k_B T} + \xi_i,$$

where ξ_i is a random number drawn from a centered Gaussian distribution with width σ_r that characterizes the quality of sampling, and $\ln(M_0)$ and Q_m are determined from the Arrhenius fit by minimizing the function

$$\chi(a,b) = \frac{1}{N_i}\sum_i \left[\ln(M_i) - a - \frac{b}{k_B T_i}\right]^2$$

that is summed over the set of N_i samples $\{M_i\}$ at temperatures $\{T_i\}$. A straightforward statistical analysis then relates the statistical error in the fitted values of $\ln(M_0)$ and Q_m to σ_r, that in turn is measured by the minimum value of the function χ. That is, $\chi_{\min} = (1-\frac{2}{N_i})\,\sigma_r^2$ gives σ_r and then the standard deviations for the Arrhenius parameters are $\sigma(Q_m) = k_B \frac{\sigma_r}{\sqrt{N_i}}[\frac{1}{\overline{x^2} - \bar{x}^2}]^{1/2}$ and $\sigma[\ln(M_0)] = \frac{\sigma_r}{\sqrt{N_i}}[\frac{\overline{x^2}}{\overline{x^2} - \bar{x}^2}]^{1/2}$ with $\overline{x^2} = \frac{1}{N_i}\sum_i \frac{1}{T_i^2}$ and $\bar{x} = \frac{1}{N_i}\sum_i \frac{1}{T_i}$.

Melting alters atomic mobility significantly, and essentially erases any vacancy that is present in the solid, so we perform two checks to ensure that the simulations are performed below the melting temperature (T_m). First, the diffusivities, when plotted as $\ln(M)$ vs $1/T$, are linear (i.e., Arrhenius) both below and above T_m but with a shift in the slope. Any deviation in slope at higher temperatures then results in a check for melting. Second, we randomly check the crystallinity of the samples by eye. We note that our samples seem to melt fairly readily, and that for the pure elements this occurs within 50 K of T_m as determined by Foiles and Adams [22]. This is in contrast to the behavior reported by de Lorenzi and Ercolessi [27], who were able to superheat their solids above T_m and continue the calculations for solid diffusivity. We also note that because of the eutectic effect, alloys may melt at a temperature significantly lower than the compositional average of the melting points of the constituent elements. The data we report below were run up to as high a temperature as possible without melting, giving an estimate (likely within 50 K) for the melting points. These are the values we use when making the comparisons using homologous temperatures.

Visually, the dominant mechanism is hopping of a nearest neighbor atom into the vacant site. Occasionally multiple atoms will move in a coordinated way, reminiscent of what de Lorenzi and Ercolessi [27] reported, but we have not studied this in detail. It is important to note that our approach using MSD makes no assumption about the nature of the diffusion, beyond that we have designed the system so that there are only single vacancies (thus excluding the possibility of vacancy clusters).

Because vacancy hopping is the dominant mechanism for evolution, our simulations could allow some degree of phase separation to occur should this be energetically favorable. This phase separation or compositional rearrangement is dependent on, and therefore secondary to, the vacancy motion itself, implying that the time scale of evolution is long enough that it should be possible to run our diffusion calculations for a reasonable time before the assumed randomness of our samples is affected. To confirm this, we calculated particle-particle correlations and found that the type-type frequencies for nearest neighbors were very close to random occupations both before and after the runs, so that we are indeed sampling properties of fully random alloys.

D. Sluggish criteria and reference diffusivities

Part of the difficulty of determining whether vacancies are "sluggish" is choosing a suitable criterion. As a practical matter there may be no single criterion suitable to all specific circumstances (that is, it may depend upon application). For our purposes of investigating a general trend we seek a *general* way of determining whether the vacancy mobility is "sluggish" or "vigorous." We first consider the problem for examining the overall self-diffusion of the alloy (that is, the diffusion of the vacancy). Later in this section we will extend the analysis to tracer diffusivities (that is, atomic diffusion analyzed element by element).

We have examined eight different criteria for evaluating sluggishness that are discussed below. In the process, we will define a way of analyzing a reference diffusivity that turns out to be very useful—beyond the evaluation of the sluggish hypothesis—to uncover some of the trends that are present in our results. In the following, M and D are the vacancy mobilities and diffusivities, and Q_f, Q_m, and $Q_d = Q_f + Q_m$ are formation, migration, and diffusion energies. The subscript i refers to values in the pure constituents, and the mean values denoted by angle brackets like $\langle Q \rangle$ are given by rule of mixtures, as explained more below. The following outline summarizes the criteria:

(1) "Just the slowest, ma'am" (at a given T)
  (a) $M < \min\{M_i\}$
  (b) $D < \min\{D_i\}$
(2) Highest activation energies
  (a) $Q_m > \max\{Q_{m,i}\}$
  (b) $Q_d > \max\{Q_{d,i}\}$
(3) Positive "excess" energy (higher than rule of mixtures)
  (a) $\Delta Q_m = Q_m(\text{alloy}) - \langle Q_m \rangle > 0$
  (b) $\Delta Q_d = Q_d(\text{alloy}) - \langle Q_d \rangle > 0$
(4) Slow by comparison to "rule of mixtures" (at a given T)
  (a) $M < \langle M \rangle$
  (b) $D < \langle D \rangle$

Criterion 1a compares the vacancy mobility in an alloy to that in the constituents: is the vacancy less mobile in the alloy than in any constituent? Criterion 1b is the same idea, but based on diffusivity. This incorporates differences in the vacancy concentration, as an alloy may have significantly fewer vacancies and so lower diffusivity. The results of these tests depend on the temperature at which the properties are evaluated.

Criterion 2a compares migration energies for the alloy to those of the constituents, while the comparison of diffusion energies is made in criterion 2b. These are independent of temperature, and while related, are not identical to 1a and 1b because of differences in the pre-exponentials.

Criteria 3a and 3b are suggested by an analogy to the rule of mixtures, by which an ideal mixture exhibits properties that are a mean of the properties of the constituents. This suggests, for example, that the migration energy of an ideal alloy should be the arithmetic mean of the migration energies of the constituents. Using the ideal alloy migration energy as a reference, we evaluate the excess migration energy as

$$\Delta Q_{m,\text{alloy}} = Q_{m,\text{alloy}} - \langle Q_m \rangle, \tag{6}$$

$$\Delta Q_{d,\text{alloy}} = Q_{d,\text{alloy}} - \langle Q_d \rangle, \tag{7}$$

where the average for energies is arithmetic:

$$\langle Q \rangle = \frac{1}{N} \sum_{i=1}^{N} Q_i. \tag{8}$$

These measures focus on the effect of alloying in comparison to the constituent properties, and thus are reasonable measures for our present investigation. Obviously, the excess migration energy or excess diffusion energy are not as physically significant as, say, the excess heat of mixing, but they nonetheless are appealing constructs and in fact turn out to provide remarkably helpful means of analyzing our results.

Because diffusion is largely dominated by the activation energy for diffusion, a negative value for this difference means that alloying has produced a medium that has faster diffusion (given the same pre-exponential) than an average of the constituents. This measure of the enhancement or reduction of diffusivity due to alloying is then done at the same absolute temperature.

The final criteria 4a and 4b are related to 3a and 3b with the rule of mixtures applied to constituent diffusivities and mobilities. Based on the expected Arrhenius behavior, the arithmetic mean of migration energies corresponds to the geometric mean of mobilities (and similarly for diffusivity):

$$\langle M \rangle = \left(\prod_{i=1}^{N} M_i \right)^{1/N}, \tag{9}$$

$$\langle D \rangle = \left(\prod_{i=1}^{N} D_i \right)^{1/N}. \tag{10}$$

This use of the rule of mixtures is a plausible hypothesis but without rigorous backing. When we apply this rule of mixtures to the results our calculations, though (in Sec. III E), we find that, when combined with the lattice mismatch parameter [Eq. (16)], it is helpful for quantitatively describing the diffusivity of the alloys we investigate.

Thus, we will use as a measure of the effect of alloying the ratio of the alloy diffusivity to the mean of the constituent diffusivities: $(D/\langle D \rangle)$. This can be decomposed into two parts: the ratio for the pre-exponential $(D_0/\langle D_0 \rangle)$ and the difference for the diffusion energy ΔQ_d. Our measure can be thought of as the "excess" value of Q away from the rule of mixtures. In this sense, these measures focus on the effect of alloying, and so are reasonable measures to use in our present investigation. We show that these mean values are in fact quite helpful in understanding the trends relating to vacancy diffusion in these alloys.

E. Using homologous temperature

To investigate the effect of using homologous temperature, we include two criteria for evaluating diffusivity—similar to the first four criteria from the previous subsection—at the melting point or scaling the energies by the melting temperature.

(1) "Just the slowest, ma'am" (at the melt or solidus temperature, called generically T_m)
  (a) $M(T_m) < \min\{M_i(T_{m,i})\}$

(b) $D(T_m) < \min\{D_i(T_{m,i})\}$ (This corresponds to Miracle [9].)

(2) Highest homologous activation energies

(a) $Q_m/T_m > \max\{Q_{m,i}/T_{m,i}\}$

(b) $Q_d/T_m > \max\{Q_{d,i}/T_{m,i}\}$ (Similar to TTY13 [6].)

Note that criterion 5b is used by Miracle [9] and criterion 6b almost corresponds to that used in TTY13 [6], except that there it is applied to tracer diffusivities. Because the melting/solidus point of the alloy is usually less than that of the constituents, it is expected that using homologous temperature should be a *less* stringent criterion than using absolute temperature (i.e., because the comparisons are done at lower temperature where overall diffusion is slower).

F. Tracer diffusivities

For tracer diffusivities, the same calculations can be done by specifying the type of atom considered, so that the mobilities are restricted to a given constituent of the alloy. Likewise, migration and diffusion energies are specific to migrating type as well as host. In calculating the excess energies (see previous subsection), as well as for comparison to experiment (see below), this involves a further calculation of the energy barrier for an atom in each of the pure constituent elements in the ideal alloy. That is, we calculate the barrier for a single atom of type A in a pure lattice of type B that begins next to a vacancy and then jumps into the vacancy. This must also include the binding energy of the impurity to the vacancy. Once this is known, we can calculate $\Delta Q^A_{\text{alloy}}$ (superscript indicates tracer of type A). An advantage of this definition for ΔQ (with the rule of mixtures as reference) is that we can compare directly to the thermochemical data for diffusion in alloys that is available for many of the binaries that we are considering. It is standard in the thermochemical analysis to fit tracer diffusivity data as a function of alloy composition to a general polynomial expansion in terms of compositions. For example, for the Au-Ni binary system the activation enthalpy for diffusivity for Au has been fitted to this function of the binary composition (using the notation of Ref. [29] that is typical of the literature):

$$\Delta G^*_{\text{Au}} = x_{\text{Au}}\Delta G^{\text{Au}}_{\text{Au}} + x_{\text{Ni}}\Delta G^{\text{Ni}}_{\text{Au}} + x_{\text{Au}}x_{\text{Ni}}\Delta^0 G^{\text{Au,Ni}}_{\text{Au}} + x_{\text{Au}}x_{\text{Ni}}(x_{\text{Au}} - x_{\text{Ni}})\Delta^1 G^{\text{Au,Ni}}_{\text{Au}}, \quad (11)$$

where the fractional compositions $x_{\text{Au}} + x_{\text{Ni}} = 1$. The first term on the right-hand side corresponds to Au diffusion in Au, the second to Au diffusion in otherwise pure Ni, and the last two terms to parameters describing diffusion across the full range of alloying. The thermochemical fitting then results in four parameters, the first of which is not specific to the Au-Ni binary. For the case of equimolar alloys, the last term becomes zero and the first two terms become an arithmetic average of the activation enthalpies in the pure constituents. Then our definition of ΔQ (i.e., comparing the activation energy in the alloy to that of the ideal composite) can be compared directly to available thermochemical data. If the agreement is perfect, we should find for a vacancy V:

$$\Delta G^{\text{Au}}_{\text{Au}} = Q_f(V \text{ in Au}) + Q_m(V \text{ in Au}) = Q_d(V \text{ in Au}), \quad (12)$$

$$\Delta G^{\text{Ni}}_{\text{Au}} = Q_f(V \text{ in Ni}) + Q_m(V \text{ trading place with Au, in otherwise pure Ni}) - Q_b(V \text{ binding to Au in otherwise pure Ni}), \quad (13)$$

$$\tfrac{1}{4}\Delta^0 G^{\text{Au,Ni}}_{\text{Au}} = \Delta Q_d(\text{Au in AuNi}), \quad (14)$$

where the last comes from evaluating Eq. (11) at 50-50 composition. We note again that the diffusion enthalpy is a combination of formation and migration. While we calculate formation and migration separately, in the thermochemical literature only the full activation enthalpies for diffusion are determined. However, we remind the reader that the EAM functions were originally fit to the vacancy formation energies available for the pure elements, and were tested successfully on the vacancy migration energies in those elements, so those are expected to be in reasonable agreement with experiment.

G. Statistical measure of properties

In the spirit of having a material formed from many constituents, we also define statistical measures of the set of constituents. For example, if we view the set of lattice constants ($\{a_{0i}\}$) in terms of a probability distribution, we can then form various moments of the distribution. The first moment of the distribution of lattice constants is the average lattice constant,

$$\overline{a_0} = \frac{1}{M}\sum_{i=1}^{M} a_{0i}. \quad (15)$$

The average is the lattice constant of the alloy from Vegard's law, and constitutes a good estimate of the actual lattice constant. The second moment, $\overline{a_0^2} = \frac{1}{M}\sum_{i=1}^{M}(a_{0i})^2$, measures the width of the distribution of lattice constants, so that the ratio of the rms (root-mean squared) to the mean is the *fractional lattice mismatch* for the alloy,

$$\delta = \frac{\sqrt{\frac{1}{M}\sum_{i=1}^{M}(a_{0i} - \bar{a}_0)^2}}{\bar{a}_0}. \quad (16)$$

This parameter is often used to place bounds on suitable candidates for high entropy alloys [30]. For the present FBD set of elements, δ ranges up to nearly 8%. For the often-studied so-called "Cantor alloy" (CrMnFeCoNi) studied in TTY13, Owen *et al.* [31] evaluate δ to be ∼1%.

III. RESULTS FOR SELF-DIFFUSION

A. Vacancy formation and migration in the six elements

We examine first the results for the six pure elements (Cu, Ag, Au, Ni, Pd, Pt). We report first formation, then migration.

The procedure for calculating vacancy formation energies in the equimolar alloys reduces for the simple case of a pure metal to the straightforward method used in FBD, and so we expect and find agreement between our present results and those in the original FBD paper.

By contrast, we note that our present method for calculating mobilities is dynamic rather than static as in FBD, and

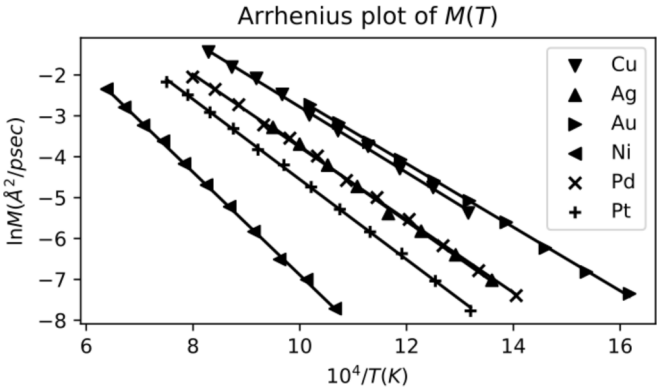

FIG. 1. Arrhenius plot [$\ln(M)$ vs $1/T$] of the vacancy mobility calculated for the six elements in the FBD set. Lines represent linear fits.

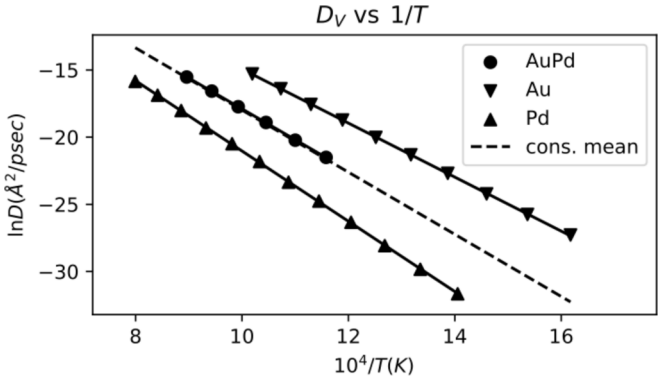

FIG. 2. Arrhenius plot of calculated self-diffusivity in Au, Pd, and (random) AuPd, with the alloy diffusivity in between and close to the mean of the constituents [Eq. (10)]. The solid lines are fits to the data, and the dashed line for the mean is computed from those fits.

so it is not necessarily expected to find agreement, but in fact we do find our dynamical results in close agreement with the static saddle-point calculations in FBD. In Fig. 1 we show the calculated mobilities for the pure metals from the FBD set (Cu, Ag, Au, Ni, Pd, Pt) at temperatures up to their respective melting points [22]. As described above, these results were calculated for cells of 108 atoms, checked against 256-atom cells, with results representing the average of 256 total runs at each temperature, each run for a diffusion length of 1 a_0. (As noted in the Methods section, the compositional homogeneity of the pure metals allows for shorter runs than the alloys.) From these we fit a line to $\ln(M)$ vs $1/T$ and extract M_0 and Q_m for each element. These results are shown in Table II, along with the saddle-point energies for the FBD functions as calculated by molecular statics (constrained optimization).

From the Arrhenius fits and error analysis discussed in the Methods section, we have determined that for the pure elements the statistical sampling errors on values of $\ln(M_0)$ and Q_m are 13% and 0.013 eV, respectively. These independent error estimates for Q_m are consistent with the errors for the elements seen in Table II (for the elements).

We find that the migration energies for all six metals correspond to the saddle-point energy for vacancy migration. Examining the energy surface for the system moving a nearest neighbor into the vacant site, we find that the energy surface for all of the FBD elements is quite simple, with the saddle point being halfway between the two lattice positions. This is in contrast to de Lorenzi and Ercolessi [27] who find that the migration energy is not equal to the saddle-point energy but differs by about 0.2 eV. In their case, the dynamical effect seems to be related to the more complex energy surface for their gold "glue" potentials. ("Glue" potentials are generically the same as EAM, but differ in some specifics.) We point out that our MD calculations are the most appropriate way to calculate the migration energy for the dynamical system.

TABLE II. Computed values for the Arrhenius constants (M_0, Q_m) for vacancy migration compared to the migration saddle-point energies from the original source [19]. (Note correction to Q published in the erratum [20].)

Element	M_0 (Å^2/psec) (this work)	Q_m (eV) (this work)	Q_m (eV) (FBD [19,20])
Cu	190	0.67	0.67
Ag	230	0.77	0.78
Au	180	0.65	0.64
Ni	290	1.05	1.06
Pd	170	0.74	0.74
Pt	190	0.82	0.82

B. Vacancy diffusivities in the 57 alloys

We present first in this subsection a selection of results for the vacancy diffusivities (combining formation and migration as described in the previous section) from the 57 equimolar alloys (15 binaries, 20 ternaries, 15 quaternaries, 6 quinaries, and one senary) that can be formed from the FBD elements. The selection is intended to show the range of behavior among the 57 alloys, where most are considered to be vigorous diffusers but a small list of 7 can reasonably be called sluggish.

We note at this point that the statistical errors in $\ln(M_0)$ and Q_m are slightly bigger for the alloys than the pure elements—28% and 0.024 eV, respectively. These errors are small enough that we can still extract meaningful trends from our calculations.

In Figs. 2 –4, we show the self-diffusivity for three binaries (AuPd, NiPt, and AgPt) along with the pure constituents for each case. The diffusivity in AuPd (Fig. 2) is moderate, in that it is sandwiched between those for Au and Pd, and is close to the mean [Eq. (10)]. Diffusion in NiPt (Fig. 3) is enhanced in that vacancies in the alloy are faster than in either Ni or Pt. Finally, diffusion in AgPt (Fig. 4) is marginally sluggish in that in the alloy the vacancies diffuse slower than in Ag or the mean of the two components, but still faster than in Pt.

In Figs. 5 and 6, the diffusivity is shown for two ternaries (AgAuNi and AgPdPt). Again, in these figures we plot the diffusivities compared to the individual constituents and their mean. The diffusivity is clearly enhanced in AgAuNi and moderately sluggish for AgPdPt.

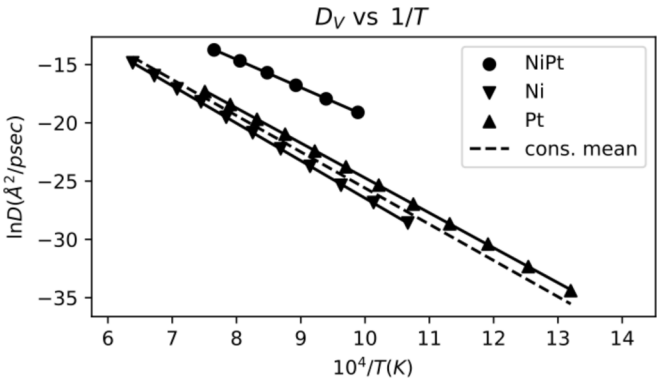

FIG. 3. Arrhenius plot of self-diffusivity in Ni, Pt, and (random) NiPt, showing enhanced diffusivity in the alloy (see Fig. 2 caption for an explanation of the lines).

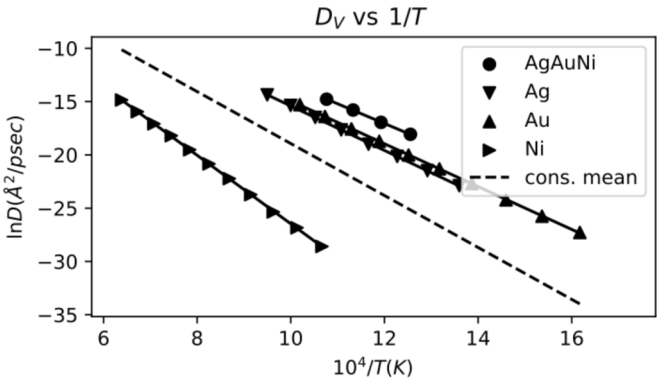

FIG. 5. Arrhenius plot for self-diffusivity of Ag, Au, Ni, and (random) AgAuNi (see Fig. 2 caption for explanation of the lines). By the criteria presented in the text, this ternary would be an example of enhanced diffusion.

In Fig. 7, we show the results for two quaternary alloys, AgAuPdPt and CuAgAuNi, with the former being slightly sluggish and the latter vigorous. In Fig. 8, we show a quinary (CuAgAuNiPd) that is vigorous, like all quinaries considered here, and the only six-component alloy in our set (CuAgAuNiPdPt), that is moderately vigorous.

In Table III, we show the classification using the various criteria described in the Methods section. Among the 63 materials considered here (6 pure elements + 57 equimolar alloys), evaluated at $T = 1000$ K, the slowest materials (in increasing order) are Ni, Pt, PdPt, AgPt, CuNi, AgPdPt, Pd, AuPdPt, AuPt, NiPt. Note that these are simple elements and binaries or ternaries; alloys with more constituents come later on the list. Also note that all alloys are faster than at least one of the constituents in pure form, e.g., PdPt, AgPt, AgPdPt, AuPdPt, AuPt, and NiPt are faster than Pt, and CuNi is faster than Ni.

As expected, the first four criteria (1a, 1b, 2a, and 2b) are more stringent than the latter four (3a, 3b, 4a, and 4b) and result in fewer alloys being classified as sluggish. The sluggish alloys are mostly binaries (five out of the 15 possible: AgAu, AgPd, AgPt, AuPd, AuPt), though there are some ternaries (four of the 20 possible: AgAuPd, AgAuPt, AgPdPt, AuPdPt) and one quaternary of the 15 possible (AgAuPdPt). It is clear from Table III that all sluggish alloys are made from the same four elements (Ag, Au, Pd, and Pt), and this will be largely explained in the next subsection. We will consider in the following a better evaluation of the magnitude of the changes in diffusivity for all the alloys, but even at this level it is clear that having many constituents alone is insufficient for sluggish diffusion.

On the other side of the spectrum, we list in Table IV those alloys that could be considered "vigorous" by reversing criteria 1a and 1b; $M > \max\{Mi\}$ and $D > \max\{Di\}$). We note that Ni is the most common constituent on this list, and Pt is the least common.

It is clear that this large set of alloys can be characterized by many differences including number of constituents, but also a wide variety of other properties like differences in cohesive energy, lattice constants, moduli, etc. Without analyzing these correlations as well, the above results are not particularly illuminating.

Furthermore, simply qualifying an alloy as sluggish or vigorous ignores things that alloys can reveal by understanding what controls diffusion. For this reason, we will next consider what properties might be correlated with diffusivity as measured relative to the constituent means.

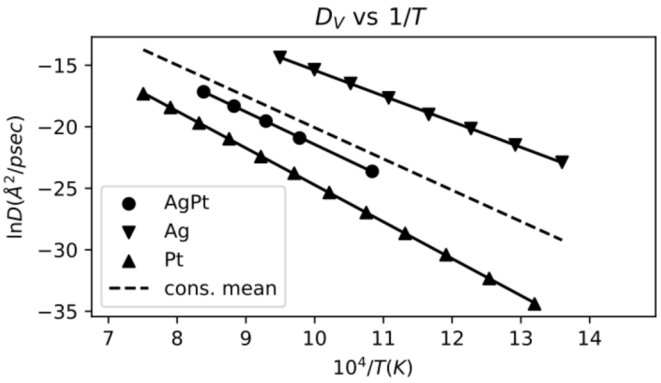

FIG. 4. Arrhenius plot of self-diffusivity in Ag, Pt, and (random) AgPt, showing slower vacancy motion in the alloy than in the mean of its constituents. Note, however, that the diffusion in pure Pt is the slowest (see Fig. 2 caption for an explanation of the line).

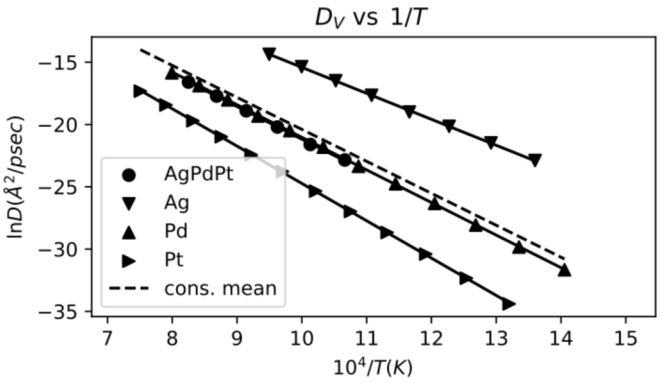

FIG. 6. Arrhenius plot for self-diffusion in Ag, Pd, Pt, and (random) AgPdPt (see Fig. 2 caption for explanation of the lines). By the criteria presented in the text, this ternary exhibits moderately sluggish diffusion.

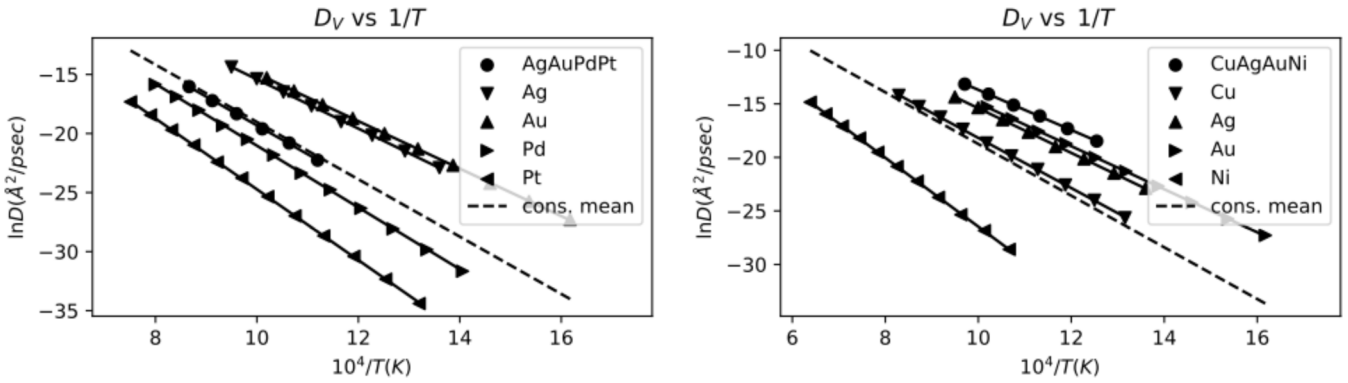

FIG. 7. Two quaternaries, one showing slightly sluggish vacancy diffusion (left) and the other enhanced (right) (see Fig. 2 caption for explanation of the lines).

C. Further analysis

While we have concluded that the presence of many components alone is insufficient for suppressed vacancy mobility, Figs. 2–8 do show some examples of alloys that are sluggish or at least moderately slow. Here we consider the possibility of correlating the diffusivity of the alloys with various constituent properties. This is useful for two reasons. First and foremost, an understanding of correlative properties may guide the theoretical investigation into root causes. Related to this, as the current calculations use the semiempirical EAM, these properties are included in the fitting of the potentials. It is then helpful to understand the connection between predictions (such as vacancy mobility in a random alloy) and training properties to help guide the empirical search for new materials.

We begin by correlating with the mean of constituent diffusivities. In the left panel of Fig. 9 we show a scatter plot of the diffusivity against the mean diffusivity of the constituents. There is considerable scatter, and the only conclusion is that $\langle D\rangle$ is close to a lower bound for D. We next investigate whether this scatter might be reduced if we take into account correlations with various properties.

The properties we consider in correlating to $D/\langle D\rangle$ are lattice constant (a_0), sublimation energy ($E_{\rm sub}$), vacancy formation energy (Q_f), vacancy migration energy (Q_m), the three cubic elastic constants (C_{11}, C_{12}, C_{44}), and (in a slightly different way) the dilute heats of mixing for the binaries. We also consider combinations of the elastic constants in the bulk modulus [$B = (C_{11} + 2C_{12})/3$], two shear moduli [$C = C_{44}$ and $C' = (C_{11} - C_{12})/2$], average shear modulus $G = (3C + 2C')/5$, and the elastic anisotropy ($A = C/C'$). In inspecting correlations, we consider the mismatch of the alloy constituents similar to the parameter δ for mismatch in lattice constants [Eq. (16)] and perform a simple Pearson linear regression of the referenced diffusivity $D/\langle D\rangle$ with the rms of each property for a given alloy. For the dilute heats of mixing, however, we correlated with the average of the two heats of mixing: A in B and B in A and only considered binary alloys. We find that the majority of these properties show no strong correlation, with the notable exception of lattice mismatch [δ, Eq. (16)], shown in Fig. 10. The figure confirms a significant correlation between the diffusivity, the mean of the constituent diffusivities, and the lattice mismatch. Figure 10 again shows that having many components is not a particularly important factor in the diffusivity, whereas lattice mismatch is very significant. It also shows that many alloys exhibit *enhanced* vacancy mobility, especially for $\delta > 0.03$. For smaller δ we see that most but not all alloys are sluggish, but only by at most a factor of 2, which is not much for diffusivity. Also, we see binaries, ternaries, and quaternaries grouped around $\delta = 0.02$ all with somewhat slower diffusion. The slowest alloy (compared to the mean of its constituents) is AgPt at $\delta = 0.02$. As pointed out by Miracle [9], the measurement of diffusion coefficients is difficult, and only differences greater than a factor of 10 should be considered relevant. While the measurement of diffusivities in simulations is more

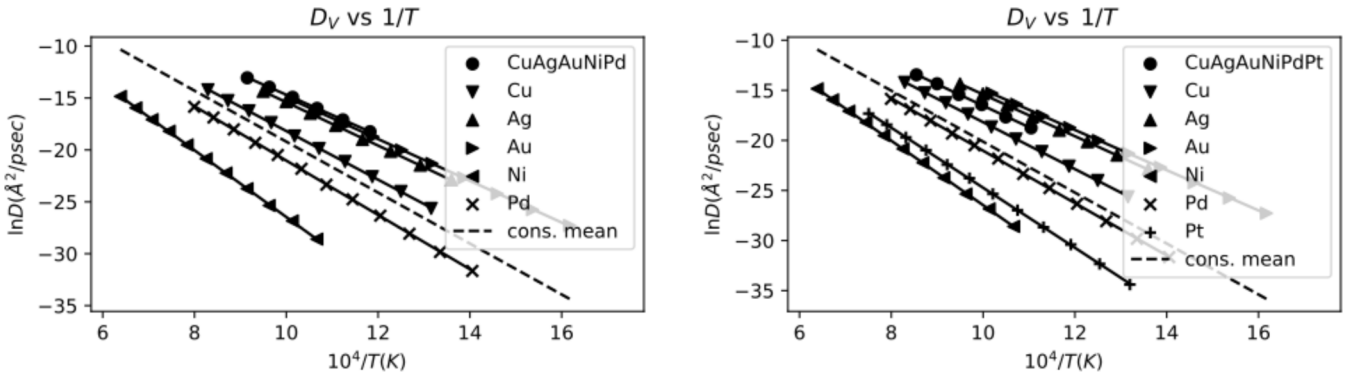

FIG. 8. A quinary and the senary alloy, both exhibiting enhanced vacancy diffusivity relative to the constituent mean.

TABLE III. Results of applying various sluggish criteria to the results of our calculations, at $T = 1000$ K (and 1500 K in parentheses if different than at 1000 K).

Criterion	Alloys meeting sluggish criterion
1a	AgPd, AgPt (also AgPdPt at 1500 K)
1b	none (AgAu only at 1500 K)
2a	AgPd, AgPt
2b	none
3a	AgPd, AgPt, AuPt, AgAuPd, AgAuPt, AgPdPt, AuPdPt, AgAuPdPt
3b	AgPd, AgPt, AgAuPt, AgPdPt, AgAuPdPt
4a	AgAu, AgPd, AgPt, AuPd, AgAuPd, AgAuPt, AgPdPt, AgAuPdPt
4b	AgAu, AgPd, AgPt, AgAuPd, AgAuPt, AgPdPt, AgAuPdPt

accurate (in the sense of smaller errors around the mean), and therefore the differences in Fig. 10 are large enough for the classification of sluggish vs enhanced, we note that none of the sluggish cases are expected to be slow enough to be experimentally distinguished.

In Fig. 10 a quadratic fit to the scatter plot gives

$$\ln(D) = \ln(\langle D\rangle) + f(\delta) \tag{17}$$

with a quadratic best fit being

$$f(\delta) = -7.14\delta + 901.8\delta^2 \tag{18}$$

In the right panel of the Fig. 9, we replot the scatter plot of the left panel but this time accounting for the correlation we have established with respect to lattice mismatch in Fig. 10. That is, when we plot $\ln(D)$ vs $\ln(\langle D\rangle) + f(\delta)$, we see a significant tightening of the correlation. A good estimate of D for an alloy is then

$$D = \langle D\rangle \exp[f(\delta)]. \tag{19}$$

This equation comes to within a factor of two for the majority (within a factor of four in the worst case) of our calculated values of diffusivities at 1500 K for the alloys. Considering that our calculated diffusivities at that temperature are spread over more than three orders of magnitude, this is a significant correlation.

We next explore in more depth the significance of the correlation in Eq. (19) by breaking the diffusivity down into preexponential and activation energy. In Fig. 11 we see that the pre-exponential trends toward suppressing vacancy diffusion with increasing lattice mismatch, but in Fig. 12 we see the *opposite* trend for the activation energy for diffusion. In fact, the overall shape of the diffusivity shown in Fig. 10 looks to be controlled by the overall behavior of the activation energy for diffusion (Fig. 12).

In Fig. 13, we further break down the activation energy for diffusion into contributions from formation and migration energies separately. The resemblance is generally consistent with the expected correlation between migration and formation energies.

Notice that because of the lattice constants of the six elements of this set, the available combinations do tend to produce more multicomponent alloys at higher δ. Specifically, there is only one quaternary at δ below 0.03 and no quinaries or senaries. Nonetheless, it is clear from comparing the alloys at higher δ that there is not much difference in the diffusivity (always in relation to the constituent mean diffusivity) among alloys with two to six components with similar values of δ. Notice also that the same trends are seen in formation and in migration energies.

Figures 10–13 also show quadratic fits as function of δ (dotted lines) to the data. In general, one can expect $\Delta Q = Q - \langle Q\rangle$ to be a function of the various parameters of the constituents, such as lattice constant, sublimation energy, etc. We start with the hypothesis that the main difference with regards to diffusion between the elements of this set is due to the lattice mismatch, and that other differences (like in cohesive energy) have a much smaller effect on the vacancy mobility. If we consider ΔQ to be a function only of δ, then a *random equimolar* alloy is symmetrical upon interchange of types, and ΔQ is an *even* function of δ, with an extremum at $\delta = 0$. With other properties being a second order effect, the type interchange symmetry will be slightly broken, resulting in an added linear dependence on δ and an extremum at $\delta \neq 0$. The fits in Figs. 10 –13 with a near-quadratic dependence with a minimum away from $\delta = 0$ suggests that lattice mismatch is indeed the dominating difference among these alloys and that other differences among the constituents are of secondary importance. We will investigate this hypothesis in more detail in a future publication.

Considered together, these results conclusively lay to rest the hypothesis of TTY13 relating complexity to sluggish diffusion in multicomponent alloys.

D. Analysis using homologous temperature

Using the criteria modified for use with homologous temperature (Sec. II E) we find that by criteria 5a and 5b *no*

TABLE IV. Results of applying various vigorous criteria to the results of our calculations. (Reversing criteria 1a and 1b: $M > \max\{M_i\}$ and $D > \max\{D_i\}$.)

Number of constituents	Vigorous alloys (reversing criteria 1a and 1b)
2	CuAg, CuAu, CuPd, AgNi, AuNi, NiPd, NiPt
3	CuAgAu, CuAgNi, CuAgPd, CuAuNi, CuAuPd, AgAuNi, AgNiPd, AgNiPt, AuNiPd, AuNiPt, NiPdPt
4	CuAgAuNi, CuAgAuPd, CuAuNiPd, CuAuNiPt, AgAuNiPd, AgNiPdPt
5	CuAgAuNiPd, CuAgAuNiPt
6	none

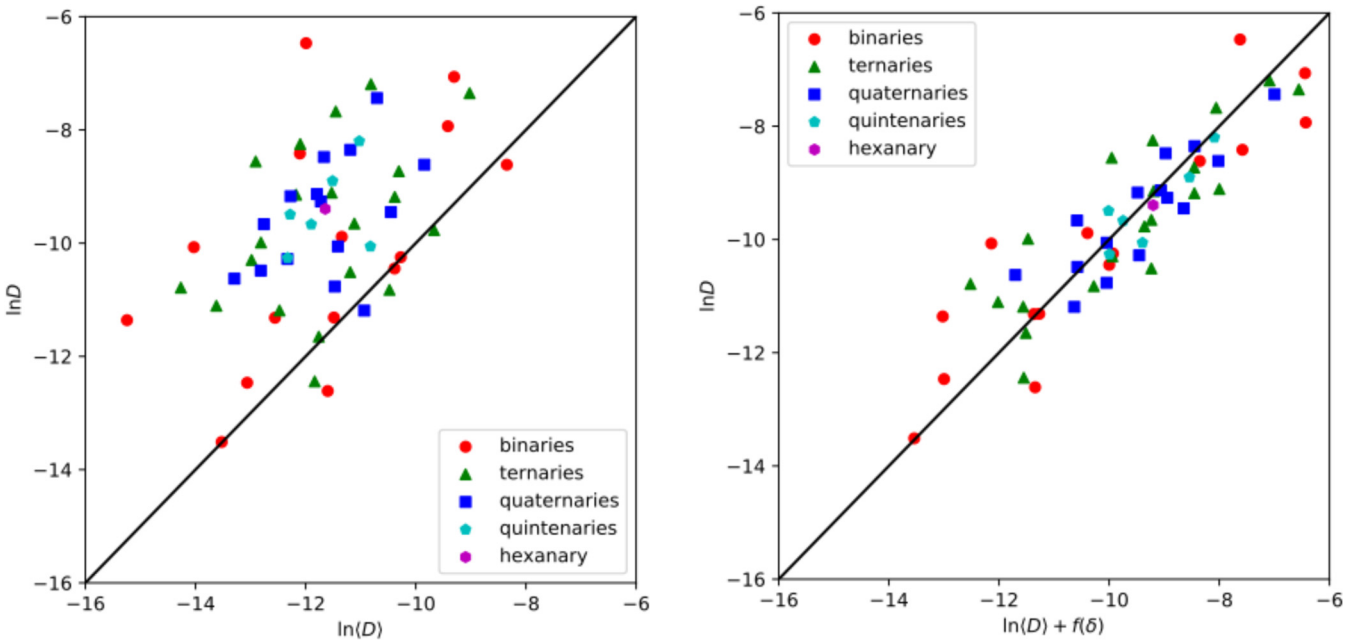

FIG. 9. Left panel: Scatter plot of $\ln(D)$ vs $\ln(\langle D\rangle)$ at $T = 1500$ K, where D is the calculated alloy diffusivity and $\langle D\rangle$ is the mean of the constituent diffusivities [Eq. (10)]. The scatter is significant, and this plot shows that $\langle D\rangle$ is close to a lower bound for D. Right panel: Scatter plot after taking into account correlation with lattice mismatch (see text). The scatter has been considerably reduced compared to the left panel. The line in both panels is 1:1.

alloys are sluggish, while by 6a and 6b we find two: AgPt and AgAuPt. On the other hand, we find even more cases of vigorous diffusion (faster than any constituents) than with absolute temperatures. Scatter plots similar to Figs. 9 and 10 with homologous values show much larger scatter, almost

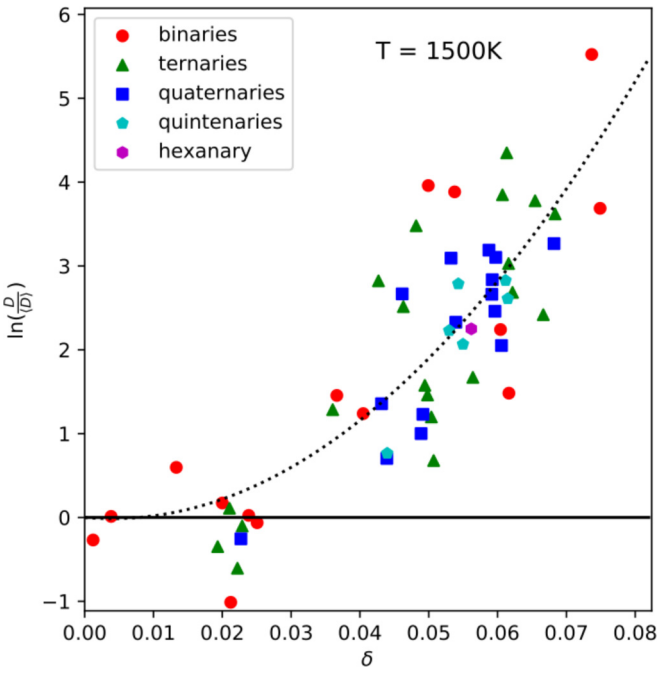

FIG. 10. Scatter plot of vacancy mobility enhancement $(D/\langle D\rangle)$ vs lattice mismatch (δ) for 57 alloys from the FBD set. The solid horizontal line separates enhanced diffusion (above) from sluggish (below). Diffusion is enhanced for most alloys, and only sluggish for some alloys with $\delta < 0.03$. The dashed line is a quadratic fit (see text).

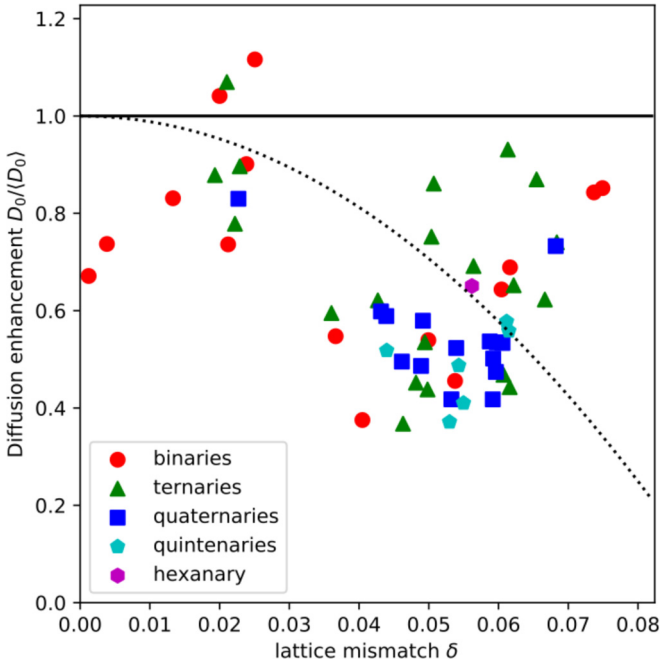

FIG. 11. Correlation of pre-exponential with lattice mismatch, showing that randomness combined with lattice mismatch tends to inhibit vacancy migration. The solid line separates enhanced (above) from sluggish (below). The trend of the pre-exponential is decidedly towards sluggish diffusion, increasing with lattice mismatch. However, this trend is overwhelmed by the opposite trend in the activation energy (Fig. 12). (The dashed line is a quadratic fit; see text).

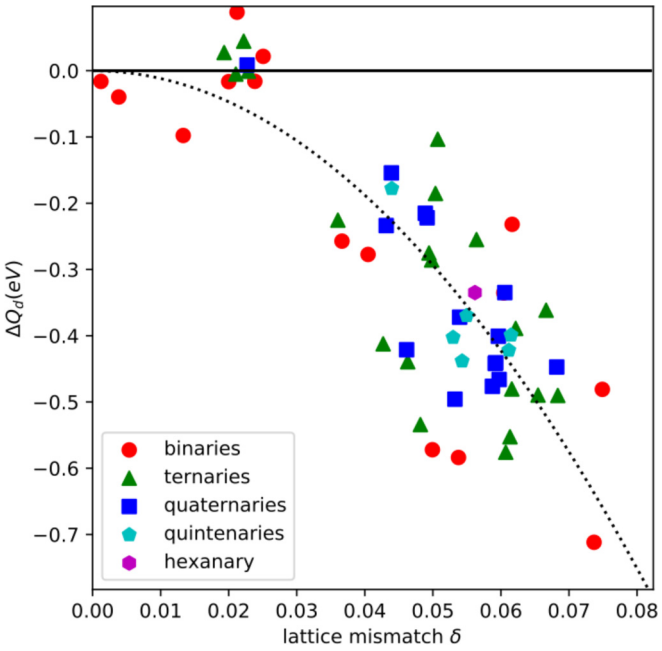

FIG. 12. Scatter plot showing the "excess" activation energy for diffusion (combined migration and formation) for alloys against lattice mismatch. The solid line divides enhanced diffusion (below the line) from sluggish (above the line). The trend correlates well with that of Fig. 10, showing that trends in the activation energy overwhelm trends in the pre-exponential shown in Fig. 11. The dotted line is a quadratic fit (see text).

obscuring the trends (and insights) we have noted in the previous subsections.

IV. RESULTS FOR PARTIAL (OR TRACER) DIFFUSIVITIES

We now analyze the same results but in terms of the diffusivity of individual constituents in the alloy (i.e., tracer diffusivities) in order to make comparisons to the available thermochemical databases. As in the above, we explore possible trends with respect to number of constituents, analyze the use of homologous temperature, and explore possible correlation with lattice mismatch.

A. Comparison to thermochemical database

As described in the Methods section, we have calculated the values for ΔQ_d [Eqs. (7) and (8)] for the elements in these alloys, and show them in Table V, compared with available thermochemical fits [like Eq. (11) evaluated at equal composition]. The table shows many cases of agreement between theory and experiment, but also individual cases of disagreement (including some with the incorrect sign). The average disagreement between our calculated values and the available experimental values is 0.27 eV. Table V also shows that for some alloys (CuAg, CuNi, AuNi) there are multiple entries in the thermochemical database with disagreement among the experimental values averaging 0.22 eV (max of 0.37 eV). Overall, we feel the agreement is reasonable, given the challenges presented by the experiments and analysis, and also the difficulties presented by these calculations. Figure 14 shows a scatter plot between the theory and experimental values showing some degree of correlation.

TABLE V. Values of ΔQ_d for various constituents in the 15 binary alloys considered in this work compared to the appropriate parameter [$\frac{1}{4}\Delta^0 G_A^{A,B}$ in Eq. (11)] obtained in thermochemical fits to experimental tracer diffusion in the same alloys (where available).

Migrant	Alloy	Theory	Experiment (Refs.)
Cu	CuAg	−0.09	−0.47, −0.26 [24,25]
Ag	CuAg	−0.31	−0.31 [24]
Cu	CuAu	−0.22	−0.19 [24,26]
Au	CuAu	−0.30	−0.24 [24,26]
Cu	CuNi	+0.05	−0.06 [23]
Ni	CuNi	−0.18	−0.27, +0.10 [23,32]
Cu	CuPd	−0.09	
Pd	CuPd	−0.31	
Cu	CuPt	−0.05	−0.14 [26]
Pt	CuPt	−0.36	+0.15 [26]
Ag	AgAu	−0.07	+0.09 [24,33]
Au	AgAu	+0.04	+0.05 [24,33]
Ag	AgNi	−0.39	
Ni	AgNi	−0.46	
Ag	AgPd	−0.04	−0.74 [34]
Pd	AgPd	+0.14	−0.02 [34]
Ag	AgPt	+0.09	
Pt	AgPt	+0.13	
Au	AuNi	−0.53	−0.51, −0.60 [35,29]
Ni	AuNi	−0.71	−0.35 [29]
Au	AuPd	+0.04	
Pd	AuPd	−0.03	
Au	AuPt	+0.08	+0.16 [34]
Pt	AuPt	−0.04	+0.39 [34]
Ni	NiPd	−0.52	
Pd	NiPd	−0.46	
Ni	NiPt	−0.45	−0.73 [36]
Pt	NiPt	−0.51	−0.78 [36]
Pd	PdPt	−0.01	
Pt	PdPt	−0.02	

B. Trends with respect to lattice mismatch

In Sec. III C we showed correlation between the calculated excess activation energy for vacancy diffusion and lattice mismatch (Fig. 12). In this section we extend the same analysis to tracer diffusivities in the binary alloys.

The left panel of Fig. 15 shows a scatter plot of the calculated excess activation energy for tracer diffusivities. The figure shows some correlation with lattice mismatch and is reminiscent of Fig. 12. In the right panel of Fig. 15 we show the same scatter plot for the corresponding parameter taken from the available thermochemical data among those same binaries. By itself, the thermochemical data would only mildly suggest a trend, but taken side by side with the clear trend in the calculated results, the experimental plot appears at least consistent with such a trend. For both theory and experiment (left and right panels) we do (independent) quadratic fits and the trend shows up the same for both, though there is more scatter in the experimental data.

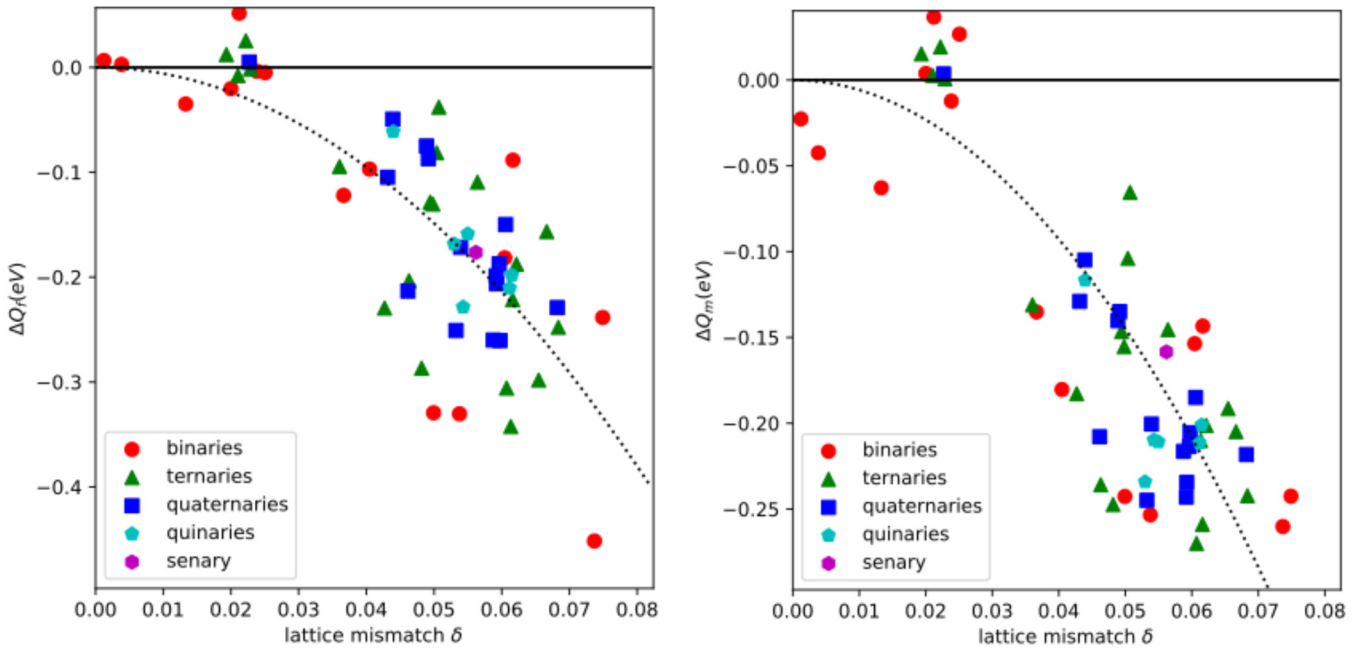

FIG. 13. Breaking down the trend in excess activation energy for diffusion correlated with lattice mismatch (Fig. 12) into contributions from formation and migration components. Left panel: Excess formation energy correlated with lattice mismatch. Right panel: Excess migration energy correlated with lattice mismatch. The dotted line is a quadratic fit given as a guide to the eye.

Figure 15 shows that the correlation with lattice mismatch found for overall vacancy diffusivity is maintained for tracer diffusivities. There is a reasonable agreement with available experimental data to support the conclusion of a trend with respect to lattice mismatch, though the experimental data alone (in that it is somewhat scattered) might not have led to this conclusion.

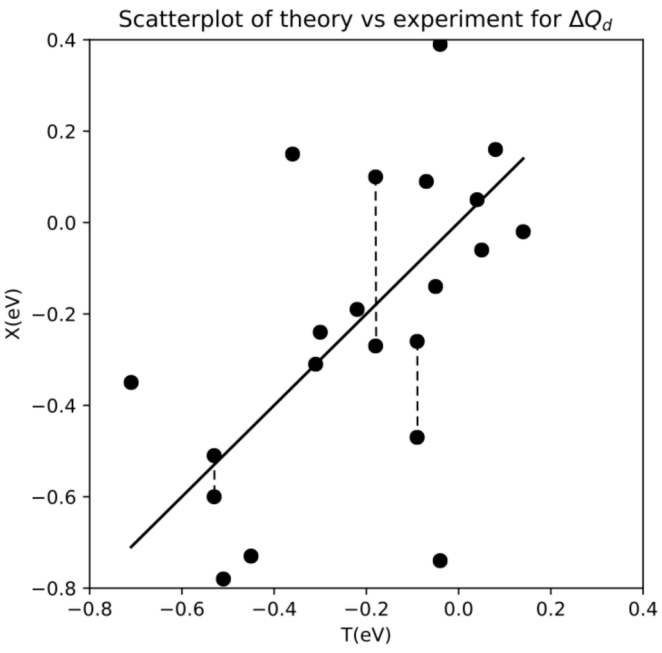

FIG. 14. Scatter plot of the experimental excess tracer activation energy X [from Eq. (11)] against the theoretical values T [given by ΔQ_d in Eqs. (7) and (8)]. All values are taken from Table V. There are three cases in Table V where two experimental values are available in the literature, and these are connected by dashed vertical lines on this plot. The diagonal line is $X = T$.

C. Trends with respect to number of constituents

Tsai, Tsai, and Yeh [6] ("TTY13" in the Introduction) found a downward trend in the homologous activation energy of tracer diffusion as a function of the number of constituents in the alloy for their data set of some alloys among Co-Cr-Fe-Mn-Ni. We have performed the same analysis for our larger set of alloys, and in Fig. 16 we show an example of the specific case of Au in various alloys containing Au. Similar plots (not shown) for the other five elements in our set lead to the same conclusion. No general trend is evident in the plot, and there is nothing to suggest a causal connection between number of constituents and the homologous activation energy. It is possible to pick out a particular sequence of alloys where the homologous activation energy has a downward trend (for example, Au, AuNi, AgAuNiPd, AgAuNiPdPt), but it is also possible to find a sequence with the opposite trend (for example, Au, CuAu, CuAuPt, CuAuNiPt). (This echoes what is pointed out by Miracle [9].) We have also made similar plots using the activation energies for diffusion (not homologous values), as well as the self-diffusion (not tracer diffusion) and in all cases we find no correlation with number of constituents. Though there are specific sequences of alloys that can be chosen to show an apparent decrease in diffusivity with increasing number of constituents, we conclude that such sequences are purely accidental. Instead, the conclusion is that there is no evidence here to suggest a *general* trend of slower diffusion with increasing number of constituents. It is worth noting that the use of homologous temperature only adds complication, without making the test for sluggishness more stringent.

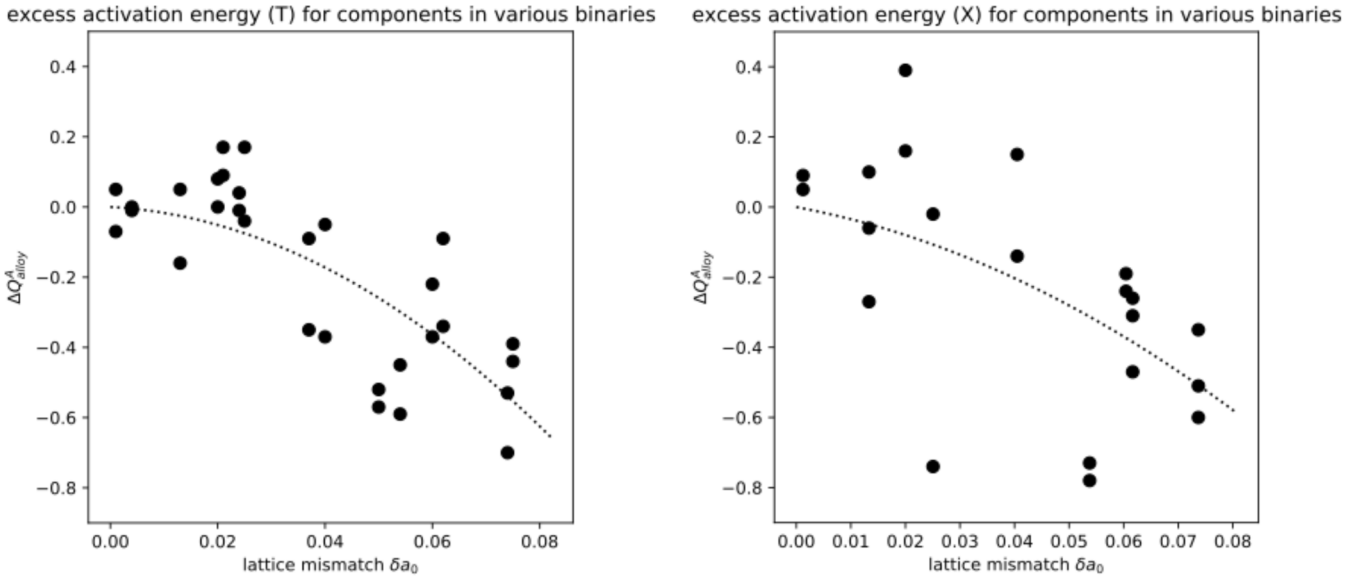

FIG. 15. Left panel: Scatter plot of the calculated excess tracer activation energy against lattice mismatch for the 15 binary alloys (two points for each alloy corresponding to the diffusion for each element in that alloy). For comparison, see Fig. 12, the same plot but for overall vacancy diffusion. A quadratic fit to the points is shown as a dashed line. Right panel: Scatter plot of the corresponding parameter taken from the available thermochemical data for the same binaries. A quadratic fit to the experimental points (similar to what is done for the left panel) is shown as a dashed line.

V. CONCLUSIONS

We report calculations of vacancy-assisted diffusion in the 57 random, equimolar alloys that can be formed from Cu, Ag, Au, Ni, Pd, and Pt, based on the well-tested functions of Foiles, Baskes, and Daw [19]. Specifically, we address two questions: (1) whether increasing the number of constituents is correlated with sluggish diffusion in these alloys, and (2) if any insight can be gained from using homologous values (e.g., evaluating diffusivity at the melt or solidus). From EAM calculations in random alloys with a single vacancy, we determine concentrations and mobilities for the vacancy, and from them the Arrhenius parameters for self-diffusion as well as tracer diffusivities. We analyze our sampling in order to determine the statistical errors of our results. Furthermore, our alloys are constructed to be as fully random as possible, and our MD calculations, while long enough to give good statistics on the diffusivity in the random alloy, are not long enough to allow any sort of short-range ordering or clustering to occur, so our results correspond indeed to properties of random alloys.

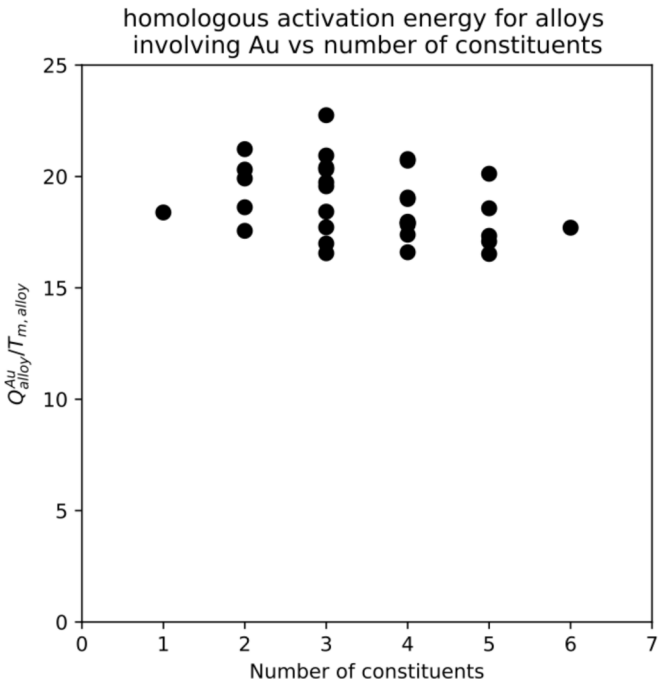

FIG. 16. Calculated homologous activation energy for tracer diffusion for Au in various alloys containing Au, as a function of the number of constituents in the alloy. Each point is a unique alloy.

We try several possible criteria for evaluating whether diffusion in an alloy is sluggish or vigorous and find only a small number in the set (two to eight out of 67 possible alloys depending on the specific criterion; see Table III) of candidates exhibiting sluggish diffusion. On the other hand, the majority of alloys considered could reasonably be said to exhibit vigorous diffusion.

We find it especially helpful to compare diffusivity in the alloy to the average diffusivity of the constituents, constructed by a in quotes to Rule of Mixtures (RoM) [Eq. (10) for diffusivity, Eq. (8) for activation energies]. Using the RoM as a benchmark for each alloy, we exhibit a further correlation with respect to the lattice mismatch of the alloy. In fact, we were able to show correlations in the diffusivity of all alloys in our set in terms of (1) the geometric mean of the constituent diffusivities, and (2) a simple function of lattice mismatch [Fig. 10 and Eq. (19)]. This simple relation accounts for the large majority of our alloy diffusivities to within a factor of 2, and to within a factor of 4 for all of our set. This is encouraging given that the diffusivities of the alloys considered here are

spread over three orders of magnitude at 1500 K. Using this measure, the few candidates for sluggish diffusion are seen to be at most a factor of 2 slower at 1500 K (too small to be resolved in most experiments), while the vigorous candidates were enhanced by one to two orders of magnitude.

We find that lattice mismatch is the principal factor controlling diffusivity (relative to RoM) for the alloys, except for the small number of sluggish alloys, all of which occur in a range of small lattice mismatch (1–3%) (see Fig. 12). However, not all alloys in this range of small lattice mismatch show sluggish diffusion; we have so far been unable to uncover the factor(s) beyond lattice mismatch that determine the small amount of sluggishness seen among some of those alloys. It is clear from Figs. 10 and 12 that the number of constituents in the alloy is largely irrelevant; alloys from two to six constituents seem to have about the same diffusivity (relative to RoM) as other alloys with the same lattice mismatch.

We find also that using homologous values disturbs (even removes) the correlation noted above. Figures similar to Figs. 10 and 12 when plotted using homologous values show much more scatter and exhibit no clear trend.

We also analyze tracer diffusivities, allowing us to compare to the available thermochemical database of diffusivities in binary alloys, and find that our calculated diffusivities are in reasonable agreement with that database (comparable to the self-consistency of that database). Again, we find that lattice mismatch seems to be the controlling factor in these results. As with the self-diffusivities, we find no significant correlation with respect to number of constituents (Fig. 16), whether or not we use homologous values. Instead, while it is possible to select sequences of alloys (selected by choosing successively more constituents to a previous alloy) that show decreasing diffusivity, these sequences are accidental (echoing Miracle [9]) it is just as easy to find sequences of alloys that show the opposite trend with increasing number of constituents.

With respect to the work of Osetsy *et al.* [15], we find nothing in our results that could be correlated with a percolation model or with anything occurring spatially different in equimolar five-component alloys than, for example, in the equimolar binaries. This is likely due to the lack of a single component that dominates the motion of a vacancy. In our calculations, the vacancy does not appear to be confined to move on the network formed by a single component, and so the system is effectively always above the percolation limit.

To summarize, we show that (1) a simple rule of mixtures, combined with (2) a simple function of lattice mismatch, can be used to account largely for the results of our calculations of diffusivities of random, equimolar FCC alloys. There remain beyond this account some other, smaller effects that we have not yet determined. For relatively small lattice mismatch (1–3%) some alloys are moderately sluggish (by at most a factor of 2 at 1500 K). There is, however, a larger number of alloys (above 3% lattice mismatch) that exhibit significantly faster diffusion (by factors of 10–100). Our analysis shows no correlation of diffusivity with the number of constituents in an alloy.

Finally, we note that all of our conclusions are based on results from a semiempirical potential that does not explicitly capture the differences in electronic structure among these metals. The insights gained here strongly invite future work based on more detailed electronic structure calculations, though it is recognized that this may be computationally challenging.

ACKNOWLEDGMENTS

This work was funded by the U.S. Department of Energy's Energy Efficiency and Renewable Energy's Advanced Manufacturing Office (DOE-EERE-AMO) through Ames Lab contract no. DE-AC02-07CH11358 and the Laboratory Directed Research and Development (LDRD) program at Sandia. Sandia National Laboratories is a multimission laboratory managed and operated by National Technology and Engineering Solutions of Sandia, LLC, a wholly owned subsidiary of Honeywell International, Inc., for the U.S. Department of Energy's National Nuclear Security Administration under Contract No. DE-NA0003525. Any subjective views or opinions that might be expressed in the paper do not necessarily represent the views of the U.S. Department of Energy or the United States Government.

[1] J. W. Yeh, S. K. Chen, S. J. Lin, J. Y. Gan, T. S. Chin, T. T. Shun, C. H. Tsau, and S. Y. Chang, Nanostructure high-entropy alloys with multiple principal elements: Novel alloy design concepts and outcomes, Adv. Eng. Mater. **6**, 299 (2004).

[2] C. J. Tong, Y. L. Chen, S. K. Chen, J. W. Yeh, T. T. Shun, C. H. Tsau, S. J. Lin, and S. Y. Chang, Microstructure characterization of AlxCoCrCuFeNi high-entropy alloy system with multiprincipal elements, Metall. Met. Trans. A **36A**, 881 (2005).

[3] J. Yeh, Recent progress in high-entropy alloys, Ann. Chim. Sci. Mater. **31**, 633 (2006).

[4] J. W. Yeh, Y. L. Chen, S. J. Lin, and S. K. Chen, High-entropy alloys – a new era of exploitation, Mater. Sci. Forum **560**, 1 (2007).

[5] J. Yeh, Alloy design strategies and future trends in high-entropy alloys JOM **65**, 1759 (2013).

[6] K. Y. Tsai, M. H. Tsai, and J. W. Yeh, Sluggish diffusion in Co-Cr-Fe-Mn-Ni high-entropy alloys, Acta Mater. **61**, 4887 (2013).

[7] TTY13 (Ref. [6]) referred to the classic work of Brown and Ashby [8] that shows some of the universal characteristics of diffusion in various structures, in pure metals and binary alloys, when scaled in terms of the homologous temperature. For example, for FCC metals and binary alloys, the homologous activation energies appear in a narrow range of values. Brown and Ashby point out that knowing this universal behavior allows for educated guesses in cases where experiments have not yet

been done. It would clearly be instructive to know if multicomponent alloys are exceptional based on this criterion.

[8] A. M. Brown and M. F. Ashby, Correlation for diffusion constants, Acta Metall. **28**, 1085 (1980).

[9] D. B. Miracle, High-entropy alloys: A current evaluation of founding ideas and core effects and exploring 'nonlinear alloys', JOM **69**, 2130 (2017).

[10] W. M. Choi, Y. H. Jo, S. S. Sohn, S. Lee, and B. J. Lee, Understanding the physical metallurgy of the CoCrFeMnNi high-entropy alloy: An atomistic simulation study, npj Comput. Mater. **4**, 1 (2018).

[11] S. Zhao, T. Egami, G. M. Stocks, and Y. Zhang, Effects of d electrons on defect properties in equiatomic NiCoCr and NiCoFeCr concentrated solid solution alloys, Phys. Rev. Mater. **2**, 013602 (2018).

[12] M. Mizuno, K. Sugita, and H. Araki, Defect energetics for diffusion in CrMnFeCoNi high-entropy alloy from first principles calculations, Comput. Mater. Sci. **170**, 109163 (2019).

[13] G. Bonny, D. Chakraborty, S. Pandey, A. Manzoor, N. Castin, S. R. Phillpot, and D. S. Aidhy, Classical interatomic potential for quaternary Ni-Fe-Cr-Pd solid solution alloys, Modell. Simul. Mater. Sci. Eng. **26**, 065014 (2018).

[14] G. Bonny, D. Terentyev, R. C. Pasionot, S. Ponce, and A. Bakaev, Interatomic potential to study plasticity in stainless steels: The FeNiCr model alloy, Modell. Simul. Mater. Sci. Eng. **19**, 085008 (2011).

[15] Y. Osetsky, L. Beland, A. Barashev, and Y. Zhang, On the existence and origin of sluggish diffusion in chemically disordered concentrated alloys, Curr. Opin. Solid State Mater. Sci. **22**, 65 (2018).

[16] S. Zhao, Y. Osetsky, and Y. Zhang, Diffusion of point defects in ordered and idsordered Ni-Fe Fe, J. Alloys Compd. **805**, 1175 (2019).

[17] M. S. Daw and M. I. Baskes, Embedded-atom method: Derivation and application to impurities, surfaces, and other defects in metals, Phys. Rev. B **29**, 6443 (1984).

[18] M. S. Daw, S. M. Foiles, and M. I. Baskes, The embedded-atom method - a review of theory and applications, Mater. Sci. Rep. **9**, 251 (1993).

[19] S. M. Foiles, M. I. Baskes, and M. S. Daw, Embedded-atom-method functions for the fcc metalls Cu, Ag, Au, Ni, Pd, Pt, and their alloys, Phys. Rev. B **33**, 7983 (1986).

[20] S. M. Foiles, M. I. Baskes, and M. S. Daw, Erratum: Embedded-atom-method functions for the fcc metals Cu, Ag, Au, Ni, Pd, Pt, and their alloys, Phys. Rev. B **37**, 10378(E) (1988).

[21] G. Neumann and C. Tujin, *Self-Diffusion and Impurity Diffusion in Pure Metals: Handbook of Experimental Data* (Elsevier, Amsterdam, 2009).

[22] S. M. Foiles and J. B. Adams, Thermodynamic properties of fcc transition metals as calculated with the embedded-atom method, Phys. Rev. B **40**, 5909 (1989).

[23] J. Wang, H. S. Liu, L. B. Liu, and Z. Jin, Assessment of diffusion mobilities in FCC Cu-Ni alloys, CALPHAD: Comput. Coupling Phase Diagrams Thermochem. **32**, 94 (2008).

[24] Y. Liu, J. Wang, Y. Du, G. Sheng, L. Zhang, and D. Liang, Atomic mobilities and diffusion characteristics for FCC Cu-Ag-Au alloys, CALPHAD: Comput. Coupling Phase Diagrams Thermochem. **35**, 314 (2011).

[25] C. Wang, L. N. Yan, J. J. Han, and X. J. Liu, Diffusion mobilities in the fcc Ag-Cu and Ag-Pd alloys, CALPHAD: Comput. Coupling Phase Diagrams Thermochem. **37**, 57 (2012).

[26] Y. Liu, L. Zhang, and D. Yu, Diffusion mobilities in fcc Cu-Au and fcc Cu-Pt alloys, J. Phase Equilib. Diffus. **30**, 136 (2009).

[27] G. de Lorenzi and F. Ercolessi, Multiple Jumps and Vacancy Diffusion in a Face- Centered-Cubic Metal, Europhys. Lett. **20**, 349 (1992).

[28] S. Plimpton, Fast Parallell Allgorithms for Short-Range Molecular Dynamics, J. Comput. Phys. **117**, 1 (1995).

[29] J. Wang, L. Liu, H. Liu, and Z. Jin, Assessment of the diffusional mobilities in the face-centred cubic Au-Ni alloys, CALPHAD: Comput. Coupling Phase Diagrams Thermochem. **31**, 249 (2007).

[30] Y. Zhang, Y. J. Zhou, J. Lin, G. L. Chen, and K. Liaw, Solid-solution phase formation rules for multi-component alloys, Adv. Eng. Mater. **10**, 534 (2008).

[31] L. Owen, E. J. Pickering, H. Y. Playford, H. J. Stone, M. G. Tucker and N. G. Jones, An assessment of the lattice strain in the CrMnFeCoNi high-entropy alloy, Acta Mater. **122**, 11 (2017).

[32] Z. Wang, L. Fang, I. Cotton, and R. Freer, Ni-Cu interdiffusion and its implication for ageing in Ni-coated Cu conductors, Mater. Sci. Eng. B **198**, 86 (2015).

[33] Y. Liu, L. Zhang, D. Yu, and Y. Ge, Study of diffusion and marker movement in fcc Ag-Au alloys, J. Phase Equilib. Diffus. **29**, 405 (2008).

[34] Y. Liu, J. Wang, Y. Du, G. Sheng, Z. Long, and L. Zhang, Phase boundary migration, Kirkendall marker shift and atomic mobilities in fcc Au-Pt alloys, CALPHAD: Comput. Coupling Phase Diagrams Thermochem. **36**, 94 (2012).

[35] A. D. Kurtz, B. L. Averbach, and M. Cohen, Self-diffusion of gold in gold-nickel alloys, Acta Metall. **3**, 442 (1955).

[36] W. Gong, L. Zhang, D. Yao, and C. Zhou, Diffusivities and atomic mobilities in fcc Ni-Pt alloys, Scr. Mater. **61**, 100 (2009).